Molecular Therapy
Nucleic Acids
Original Article

# circSETD3 Contributes to Acquired Resistance to Gefitinib in Non-Small-Cell Lung Cancer by Targeting the miR-520h/ABCG2 Pathway

Yutang Huang,[1,4] Yi Dai,[1,2,4] Chunjie Wen,[1] Shuai He,[1] Jingjing Shi,[1] Dezhang Zhao,[1] Lanxiang Wu,[1] and Honghao Zhou[1,3]

[1]Institute of Life Sciences, Chongqing Medical University, Chongqing 400016, China; [2]Wangjia Community Health Service Center, Chongqing 401120, China; [3]Pharmacogenetics Research Institute, Institute of Clinical Pharmacology, Central South University, Changsha 410078, China

**Gefitinib is a first-line treatment for patients with non-small-cell lung cancer (NSCLC), but acquired resistance is a major obstacle to its therapeutic efficacy, and the underlying mechanisms are not fully elucidated. Recent studies have indicated that circular RNAs play a crucial role in chemoresistance, but their expression and function in NSCLC cells with acquired resistance to gefitinib are largely unknown. In this study, we determined that circSETD3 was significantly upregulated in gefitinib-resistant NSCLC cell lines and the plasma of gefitinib-resistant NSCLC patients. circSETD3 markedly decreased the gefitinib sensitivity of NSCLC cells both *in vitro* and in nude mice xenografts. It could directly bind to miR-520h and lead to the upregulation of ATP-binding cassette subfamily G member 2 (ABCG2), an efflux transporter of gefitinib, resulting in a reduced intracellular gefitinib concentration. Moreover, we reported that the downregulation of serine/arginine splicing factor 1 (SRSF1) contributed to, at least in part, the increased expression of circSETD3 in NSCLC cells with acquired resistance to gefitinib. Taken together, our findings indicated that circSETD3 may serve as a prognostic biomarker and a potential therapeutic target for acquired resistance to gefitinib in NSCLC.**

## INTRODUCTION

Lung cancer is the most commonly diagnosed cancer and remains the leading cause of cancer death worldwide.[1] About 80%–85% of lung cancer is non-small-cell lung cancer (NSCLC), with a 5-year survival rate of only 16%.[2,3] In a vast majority of NSCLC tumors, the epidermal growth factor receptor (EGFR) has been found overexpressed, resulting in EGFR pathway overactivation, which leads to cellular proliferation, differentiation, and survival in the lung.[4–6] In July 2015, the US Food and Drug Administration (FDA) approved gefitinib for the first-line treatment of advanced NSCLC, and it is currently used as first-line therapy for NSCLC patients with a sensitizing EGFR mutation.[7] Unfortunately, despite initial and often dramatic responses of gefitinib treatment, nearly all patients will eventually develop acquired resistance after 10–14 months.[8] Although a number of mechanisms have been elucidated, such as EGFR T790M mutation and MET amplification, in up to 30% of patients the underlying mechanisms still remain unknown.[9,10] Moreover, a useful biomarker is highly and urgently needed to monitor the clinical response to gefitinib therapy.

Circular RNAs (circRNAs) are a class of non-coding RNAs that form covalently closed continuous loop structures.[11] The unique circular structure makes circRNAs more stable and resistant to exonucleases (e.g., RNase R).[11] In addition, circRNAs are often expressed in a tissue- and developmental stage-specific manner, and they are abundant in various tissues and body fluids such as blood, plasma, and serum.[12] These characteristics of circRNAs make them an ideal biomarker for cancer and other diseases.[12] Functional studies have strongly implicated that circRNAs are involved in gene expression regulation at the transcriptional, post-transcriptional, and translational levels and exert multiple physiological effects.[13] Recently, accumulating evidence suggests that circRNAs are involved in acquired chemotherapy resistance. For example, circAKT3 and hsa_circ_0081143 contribute to the acquired resistance to cisplatin in gastric cancer, circPVT1 mediates doxorubicin and cisplatin resistance in osteosarcoma cells, and circ_100053 plays a key role in imatinib resistance in chronic myeloid leukemia.[14–17] However, the function of circRNAs in acquired resistance to gefitinib in NSCLC has not been clearly elucidated so far.

In the present study, we found that circSETD3 (hsa_circ_0000567) was significantly upregulated in both gefitinib-resistant NSCLC cell lines and the plasma of gefitinib-resistant NSCLC patients. circSETD3 reduced gefitinib sensitivity by sponging miR-520h, thereby leading to increased expression of ATP-binding cassette subfamily G member 2 (ABCG2) and decreased intracellular gefitinib accumulation. Previous reports have shown that miR-520h is negatively related to the tumorigenesis of NSCLC, and, as a gefitinib efflux

Received 16 July 2020; accepted 21 July 2020;
https://doi.org/10.1016/j.omtn.2020.07.027.

[4]These authors contributed equally to this work.

**Correspondence:** Lanxiang Wu, Institute of Life Sciences, Chongqing Medical University, Chongqing 400016, China.
**E-mail:** lxwu@cqmu.edu.cn

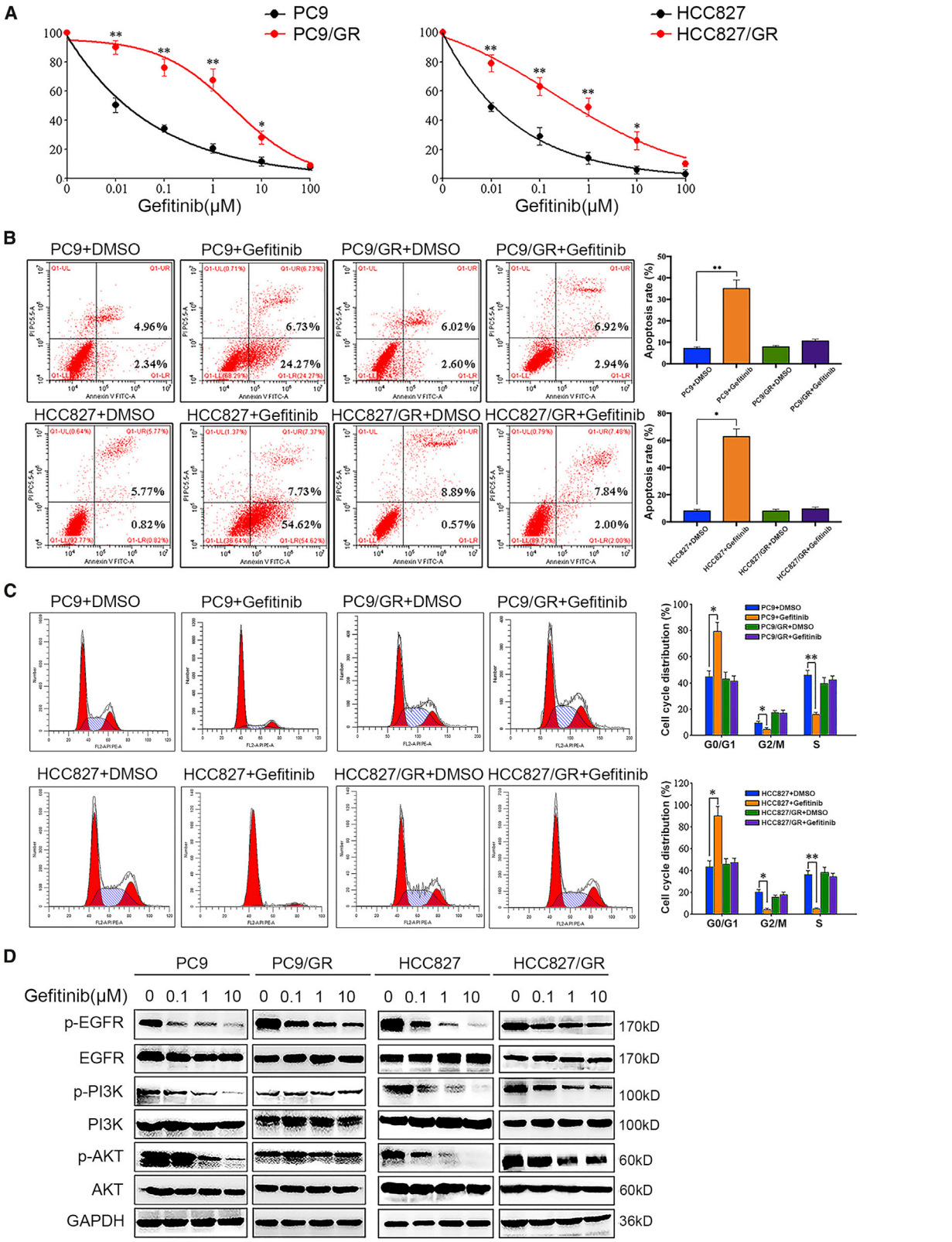


*(legend on next page)*

transporter, ABCG2 can decrease the intracellular concentration of gefitinib in NSCLC cells.[18–20] Furthermore, we revealed that the serine/arginine splicing factor 1 (SRSF1) was responsible for the upregulation of circSETD3 in NSCLC cells with acquired resistance to gefitinib. Also, previous research has found that SRSF1 is closely related to the tumorigenesis and chemoresistance in NSCLC.[21]

## RESULTS

### circRNA Expression Profiles in Gefitinib-Sensitive and -Resistant NSCLC Cell Lines

We first established the acquired gefitinib-resistant NSCLC cell sublines PC9/GR and HCC827/GR, which were derived from the parental PC9 and HCC827 cell lines and were free from EGFR T790M mutation and MET amplification.[22] Results of a Cell Counting Kit-8 (CCK-8) assay showed that the 50% inhibitory concentration ($IC_{50}$) value for gefitinib in PC9/GR cells was 1.77 μM, with a 35.40-fold increase relative to that in PC9 cells (0.05 μM), and the $IC_{50}$ value for gefitinib in HCC827/GR cells was 0.72 μM, with a 21.86-fold increase relative to that in HCC827 cells (0.03 μM) (Figure 1A). Additionally, after 1 μM gefitinib treatment, PC9 and HCC827 cells exhibited both apoptosis and $G_1$ cell cycle arrest, but PC9/GR and HCC827/GR cells were not affected (Figures 1B and 1C). Moreover, unlike their parental cells, PC9/GR and HCC827/GR cells maintained high phosphorylation levels of EGFR and downstream signaling components even following treatment with 10 μM gefitinib (Figure 1D). These results confirmed that our gefitinib-resistant NSCLC cell lines were well established.

The differentially expressed circRNAs in these cells were then examined using RNA sequencing (RNA-seq), which were shown in volcanic map (Figure 2A). A total of 51 circRNAs were differentially expressed between PC9 and PC9/GR cells, consisting of 17 upregulated and 34 downregulated circRNAs. Also, 94 circRNAs were differentially expressed between HCC827 and HCC827/GR cells, consisting of 32 upregulated and 62 downregulated circRNAs (Tables S1 and S2). Among them, eight circRNAs were altered in both two paired cell lines with the same trend, and their expression levels were verified by quantitative real-time PCR (Figures 2B and 2C).

### Upregulated circSETD3 Reduces Sensitivity to Gefitinib in NSCLC Cells

According to the results mentioned above, one of the most differentially expressed circRNAs, circSETD3 (hsa_circ_0000567), which is derived from exons 2–6 of the SET domain-containing 3 (SETD3) gene, was selected for further investigation. Its genomic structure is shown in Figure 3A. The distinct product of the expected size was amplified using outward-facing primers and confirmed by Sanger sequencing (Figure 3B). After RNase R treatment, the abundance of circSETD3 showed no significant decrease, while the linear SETD3 mRNA showed a marked reduction, which further confirmed that this RNA species exists in a circular form (Figure 3C; Figure S1). Moreover, we also investigated the stability and localization of circSETD3. After treatment with 2 μg/mL actinomycin D, an inhibitor of transcription, circSETD3 was highly stable, with a transcript half-life that exceeded 24 h, whereas the linear SETD3 mRNA exhibited a half-life of less than 8 h (Figure 3D). Quantitative real-time PCR analysis of nuclear and cytoplasmic expression demonstrated that the circSETD3 preferentially localized in the cytoplasm (Figure 3E).

We further determined the expression levels of circSETD3 in cultured gefitinib-sensitive and -resistant NSCLC cells, as well as in the plasma of gefitinib-sensitive and -resistant NSCLC patients. Compared to parental sensitive cells, significantly elevated expression of circSETD3 was observed not only in the whole-cell lysates, but also in the culture supernatants of PC9/GR and HCC827/GR cells (Figure 3F). Similarly, the level of circSETD3 in the plasma of NSCLC patients with acquired resistance to gefitinib was about 13.01-fold higher than that of gefitinib-sensitive patients (Figures 3G and 3H). These data provide evidence that circSETD3 is upregulated in NSCLC cells with acquired resistance to gefitinib both *in vitro* and *in vivo*, and is a potential biomarker for resistance to gefitinib therapy.

To study the influence of circSETD3 on gefitinib sensitivity in NSCLC cells, we modulated the expression level of circSETD3 either by overexpression in gefitinib-sensitive cells, or knockdown in gefitinib-resistant cells (Figures 4A and 4D). circSETD3 overexpression significantly upregulated the cell survival rate after various concentrations (0.01, 0.1, 1, 10, and 100 μM) of gefitinib exposure for 48 h, and the $IC_{50}$ values showed a 44.32- and 9.79-fold increase in PC9 and HCC827 cells, respectively (Figure 4B). However, the $IC_{50}$ values were reduced by 61.41% and 56.57% in PC9/GR and HCC827/GR cells after circSETD3 knockdown (Figure 4E). Additionally, after circSETD3 overexpression, gefitinib-induced apoptosis decreased from 40.73% to 16.25% in PC9 cells, and from 72.52% to 30.40% in HCC827 cells after 1 μM gefitinib exposure for 48 h (Figure 4C), whereas after circSETD3 knockdown, the gefitinib-induced apoptosis rate showed a 2.69-fold increase in PC9/GR cells and a 3.47-fold increase in HCC827/GR cells after 1 μM gefitinib exposure for 48 h (Figure 4F). Collectively, these data suggest that circSETD3 can significantly reduce the gefitinib sensitivity in NSCLC cells and is a potential target for overcoming gefitinib resistance.

Considering that the epithelial-mesenchymal transition (EMT) and minor subpopulations of cancer stem cells (CSCs) have been reported to associated with acquired resistance of gefitinib in NSCLC,[23,24] we used qRT-PCR to study the effect of circSETD3 on the expression

**Figure 1. Characterization of Gefitinib-Resistant Cell Lines PC9/GR and HCC827/GR**

(A) Cell viability of gefitinib-sensitive and -resistant cells exposed to various concentrations of gefitinib for 48 h. (B) Cell apoptosis of gefitinib-sensitive and -resistant cells after 1 μM gefitinib exposure for 48 h. (C) Cell cycle distribution of gefitinib-sensitive and -resistant cells after 1 μM gefitinib exposure for 48 h. (D) Activation of the EGFR signaling pathway in gefitinib-sensitive and -resistant cells after 1 μM gefitinib exposure for 48 h. *$p < 0.05$, **$p < 0.01$.

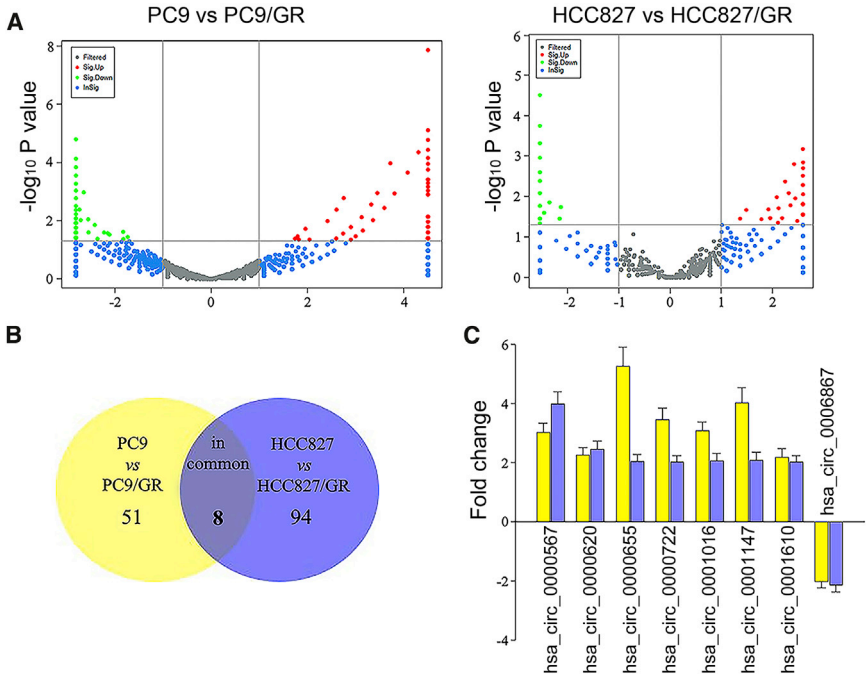


**Figure 2. Differentially Expressed circRNAs between Gefitinib-Sensitive and -Resistant NSCLC Cell Lines**

(A) Volcano plots show the differential circRNAs expression profiling between gefitinib-sensitive and -resistant NSCLC cell lines. (B) Venn diagram shows the number of differentially expressed circRNAs overlapped between two comparisons. (C) Quantitative real-time PCR validation of expression of the eight selected circRNAs.

of EMT markers (vimentin, N-cadherin, E-cadherin, and keratin 18) and stemness-related markers (CD133, OCT4, NANOG, and SOX2). Our results showed that there were no significant differences in these markers after circSETD3-overexpression plasmid (OE-circSETD3) and circSETD3-short hairpin RNA (shRNA) (sh-circSETD3) (Figure S2), which indicates that the function of circSETD3 in gefitinib resistance was irrelevant with EMT or stem cell properties in NSCLC.

### circSETD3 Acts as a Sponge for miR-520h

Given that exonic circRNAs localized in the cytoplasm can act as a microRNA (miRNA) sponge to regulate gene expression,[25] we next explored the miRNAs that could potentially interact with circSETD3, as well as their targeting genes. Using online bioinformatics databases (TargetScan, DIANA Tools, miRanda, and Circinteractome), we found that circSETD3 was potentially targeted by many miRNAs, and the five miRNAs with the highest interaction scores were miR-520h, miR-1236, miR-191, miR-149, and miR-421. Their potentially targeting genes were also predicted. Then, we used Cytoscape software to delineate the interaction network of circSETD3-miRNAs-target genes (Figure 5A). Among these miRNAs, we have significant interest in miR-520h, which has been reported to be associated with cancer progression, metastasis, as well as an anticancer drug response.[26–28]

We then observed the interaction between circSETD3 and miR-520h using a luciferase reporter system. Our results showed that miR-520h could interact with circSETD3 via a complementary seed region (Figures 5B and 5C). Moreover, a significantly reduced level of miR-520h was found in gefitinib-resistant NSCLC cells compared with their parental sensitive cells (Figure 5D). Overexpression of circSETD3 in PC9 and HCC827 cells markedly decreased the miR-520h level, whereas circSETD3 knockdown in PC9/GR and HCC827/GR cells exhibited an opposite effect (Figures 5E and 5F). However, miR-520h failed to influence the expression of circSETD3 (Figure 5G). These results imply that circSETD3 directly binds to miR-520h and acts as a miR-520h sponge.

Among the target genes in Figure 5A, we have significant interest in ABCG2, a member of the ATP-binding cassette family. Previous studies have reported that ABCG2 can decrease the intracellular accumulation of gefitinib in NSCLC cells and plays an important role in acquired resistance to gefitinib in NSCLC.[19,20] Also, previous studies have reported that miR-520h can suppress the expression of ABCG2 by binding to its 3′ UTR region.[29] Consistent with previous observations, we also found that miR-520h significantly inhibited the expression of ABCG2 in NSCLC cells, which could be rescued by a miR-520h inhibitor (Figures 5H–5J).

### circSETD3 Upregulates the Expression and Function of ABCG2

In order to further explore the functional mechanisms of circSETD3 in gefitinib resistance, we observed its influence on ABCG2 expression and efflux activity. Our results showed that circSETD3 could upregulate the luciferase activity of the reporter containing the wild-type ABCG2 3′ UTR sequence in HEK293 cells, which was remarkably suppressed by the miR-520h mimic. However, these effects were not shown in the mutant group (Figure 6A). Accordingly, circSETD3 overexpression significantly upregulated the ABCG2 level in PC9 and HCC827 cells, which could be abolished by miR-520h mimic (Figures 6B and 6D). However, circSETD3 knockdown remarkably downregulated the ABCG2 levels in PC9/GR and HCC827/GR cells, which could be rescued by the miR-520h inhibitor (Figures 6C and 6E). These data indicate that circSETD3 can abolish the inhibitory effect of miR-520h on ABCG2 expression.

It is well known that gefitinib is a substrate of ABCG2 at clinically relevant concentrations.[30] We therefore speculated that the contribution of circSETD3 to gefitinib resistance might be, at least partially, owing to the enhancement of ABCG2-mediated gefitinib efflux. We first evaluated the impact of circSETD3 on intracellular accumulation

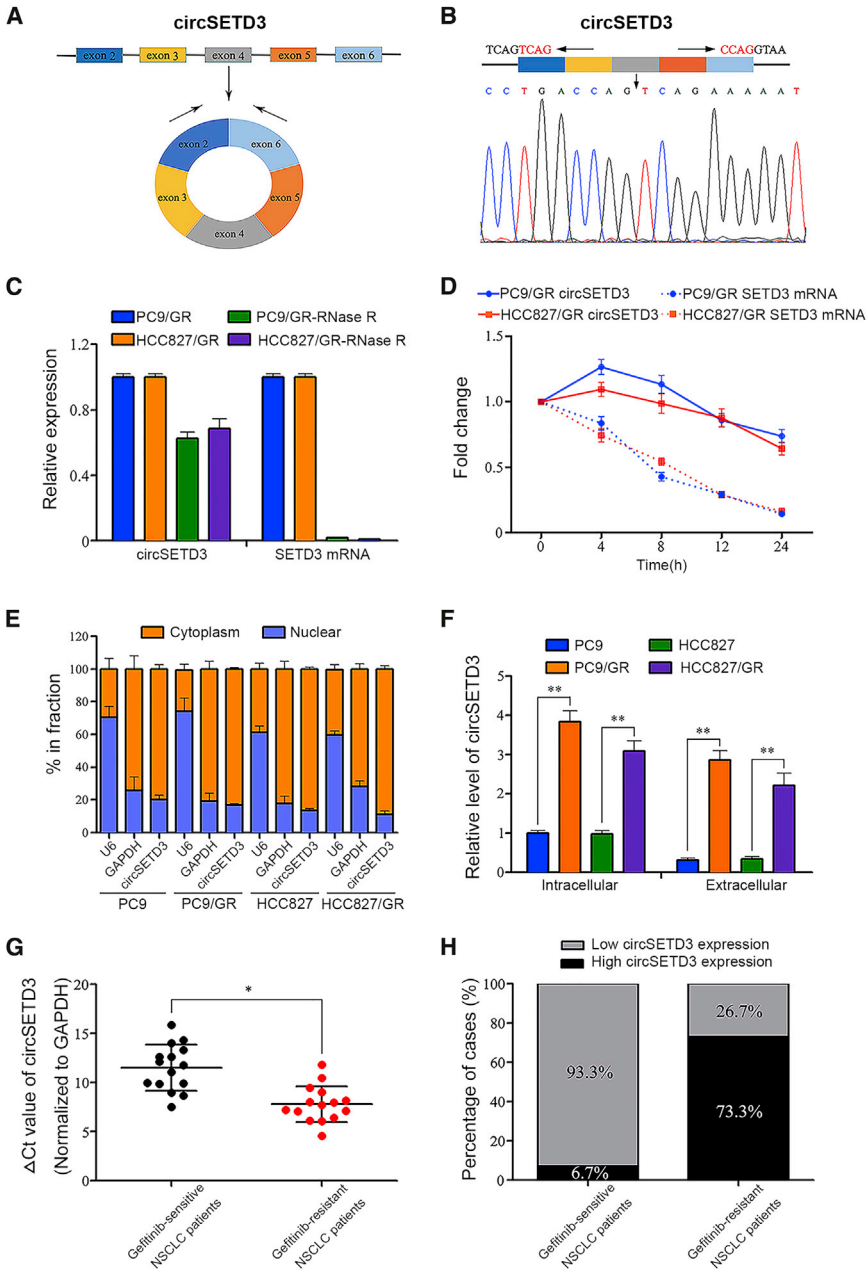


**Figure 3. The Biological Structure of circSETD3**

(A) Schematics show that circSETD3 was derived from exons 2–6 of the *SETD3* gene. (B) The amplification products of circSETD3 were confirmed by Sanger sequencing. (C) The abundance of circSETD3 and linear *SETD3* mRNA in NSCLC cells treated with RNase R (see also Figure S1). (D) The expression of circSETD3 and linear *SETD3* mRNA in NSCLC cells treated with actinomycin D. (E) The expression of circSETD3 in either the cytoplasm or nucleus of NSCLC cell lines. (F) The expression of circSETD3 in both the whole-cell lysates and the culture supernatants of gefitinib-sensitive and -resistant NSCLC cell lines. (G) The expression of circSETD3 in the plasma of gefitinib-sensitive and -resistant NSCLC patients. (H) Distribution of circSETD3 expression in the plasma of gefitinib-sensitive and -resistant NSCLC patients. *p < 0.05, **p < 0.01.

of Hoechst 33342, a typical substrate of ABCG2.[31] We found that, in PC9 cells, circSETD3 overexpression caused a 36.8% reduction in the intracellular Hoechst 33342 concentration, which was completely reversed by Ko143, an ABCG2 inhibitor.[32] However, in PC9/GR cells, circSETD3 knockdown led to about a 2.6-fold increase in Hoechst 33342 accumulation, which was completely rescued by ABCG2 overexpression (Figure 6F). Consistent with these results, the level of circSETD3 was also inversely related to the intracellular concentration of gefitinib (Figure 6G). These results suggest that circSETD3 enhances the expression and function of ABCG2 by sponging miR-520h, resulting in decreased intracellular accumulation of gefitinib and reduced gefitinib sensitivity in NSCLC cells.

### circSETD3 Is Responsible for the Gefitinib Resistance in NSCLC Cells *In Vivo*

To determine whether circSETD3 influences gefitinib sensitivity in NSCLC cells *in vivo*, PC9 xenograft models were established. Although the average body weight of mice showed no significant difference among groups (Figure 7A), circSETD3 was shown to significantly increase the tumor volume and tumor weight (Figures 7B–7D). H&E staining in xenograft models showed that circSETD3 increased the malignant degree of tumors (Figure 7E). Immunohistochemical staining of Ki-67 and ABCG2 in xenograft models showed that circSETD3 enhanced the expression of Ki-67, a well-known proliferation marker, as well as ABCG2 (Figures 7F and 7G). According with our results *in vitro*, circSETD3 increased the phosphorylation levels of EGFR and downstream signaling components in NSCLC xenograft mice models (Figure S3). These results suggest that circSETD3 can suppress the sensitivity of NSCLC cells to gefitinib *in vivo*, and inhibition of circSETD3 expression can partially restore the gefitinib sensitivity.

### circSETD3 Expression Is Regulated by SRSF1 in NSCLC Cells

Finally, we explored the potential mechanism of circSETD3 upregulation in gefitinib-resistant NSCLC cells. Previous research has shown that for most host genes, there is a balance between circular and linear RNA biogenesis.[33] Functional dysregulation of some splicing factors may be involved in the perturbation of this balance and can induce a change in circRNAs expression.[34] Therefore, we evaluated the levels

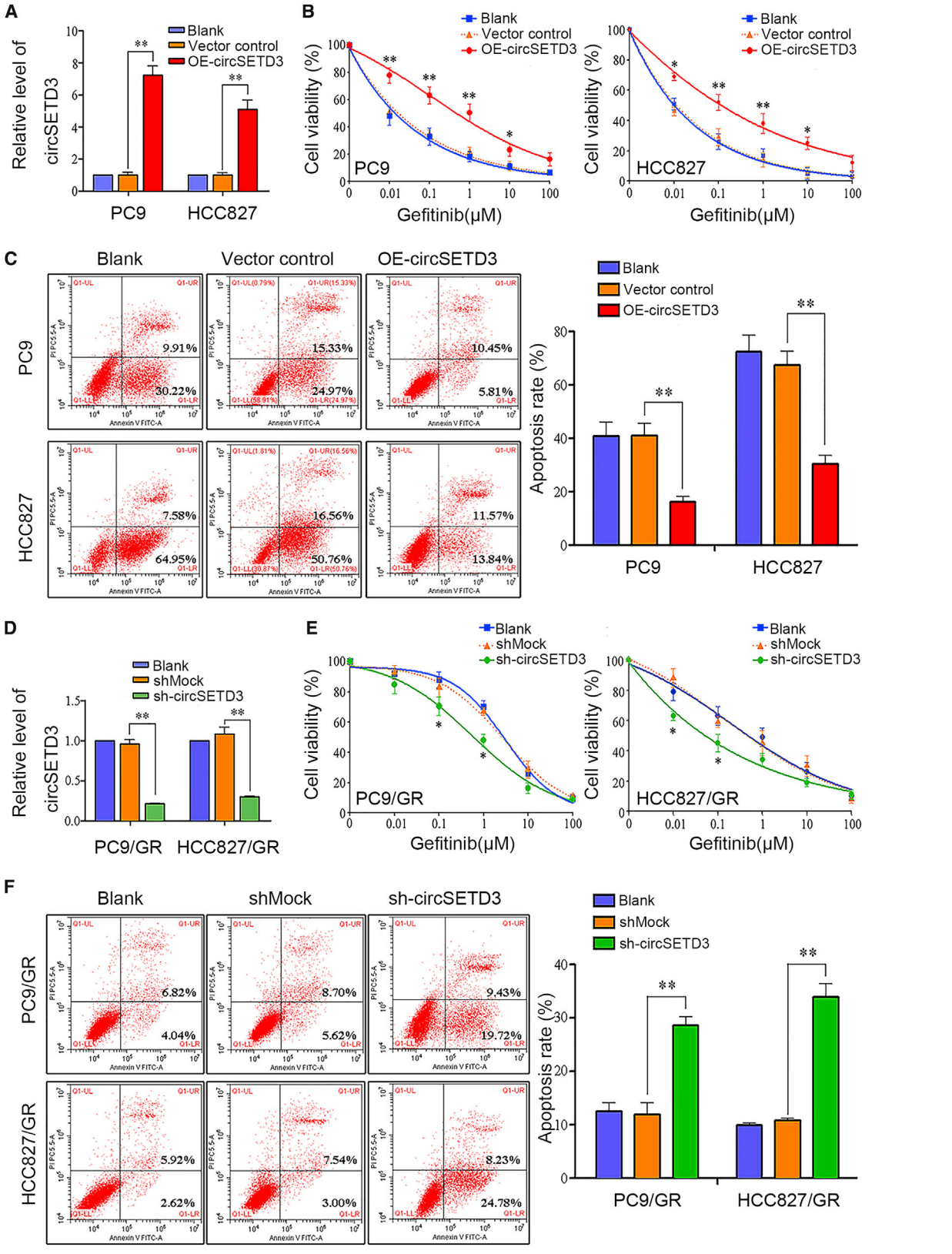


*(legend on next page)*

of *SETD3* precursor mRNA (pre-mRNA) and linear *SETD3* mRNA in all cell lines. The *SETD3* pre-mRNA level showed no difference, but the linear *SETD3* mRNA was markedly decreased in gefitinib-resistant cells (Figure 8A). Then, we selected 20 differentially expressed splicing factors between gefitinib-sensitive and -resistant cells based on RNA-seq results and verified their expression by quantitative real-time PCR (Figures 8B and 8C). We chose three common significantly downregulated splicing factors, i.e., HNRNPK, HNRNPH1, and SRSF1, for further study. After knocking down these splicing factors, we found that only SRSF1 showed significant influence on the circSETD3/SETD3 balance (Figure S4). Then, SRSF1 was chosen for further study. In NSCLC cells, knockdown of SRSF1 resulted in an increase in circSETD3 levels, as well as a decrease in linear *SETD3* mRNA expression. However, overexpression of SRSF1 led to a decrease in circSETD3 levels and an increase in linear *SETD3* mRNA expression (Figures 8D and 8E). Taken together, these results suggest that SRSF1 is responsible for the upregulation of circSETD3 in gefitinib-resistant NSCLC cells.

## DISCUSSION

In this study, we present the first study investigating the function of circRNAs in acquired resistance to gefitinib in NSCLC. First, we identified that circSETD3 was significantly upregulated in NSCLC cell lines as well as in the plasma of patients with acquired resistance to gefitinib. Recent studies of colorectal cancer (CRC) and hepatocellular carcinoma (HCC) have shown that circSETD3 was downregulated in these tumor tissues, and its expression was negatively related to tumor size and differentiation.[35,36] Thus, circSETD3 may play an unignorable role in the regulation of proliferation, differentiation, and chemosensitivity of tumor cells. Considering that circSETD3 is localized in the cytoplasm, we suppose it may act as a scaffold to modulate the function of multiple molecules. It is not surprising that it plays a distinct role in different types of tumors and under different circumstances. According to our *in vitro* and mouse xenograft studies, circSETD3 could significantly decrease the sensitivity of NSCLC cells to gefitinib. Downregulation of circSETD3 expression could markedly increase the gefitinib sensitivity in gefitinib-resistant NSCLC cells, but it could not bring back these resistant cell lines to the sensitive level of their parental sensitive cell lines. This happens because the acquired gefitinib resistance is a multi-factorial phenomenon, and some of the mechanisms are still unclear. Therefore, the influence of other mechanisms cannot be ruled out in this study.

Second, we found that the influence of circSETD3 on gefitinib sensitivity was mediated at least partially by targeting the miR-520h/ABCG2 pathway. As a member of the miR-520 family, miR-520h has been reported to play an essential role in the growth, invasion, migration, and chemoresistance of various cancer cells through targeting multiple molecules. For example, miR-520h enhances cell proliferation, migration, and invasion in epithelial ovarian cancer cells by targeting Smad7.[28] It also influences cell sensitivity to doxorubicin and paclitaxel by targeting histone deacetylase 1 (HDAC1) and death-associated protein kinase 2 (DAPK2) in gastric and breast cancer cells, respectively.[26,27] ABCG2 is also a direct target of miR-520h.[29] It can actively pump out of a variety of substrates from cells, including some anti-cancer drugs such as doxorubicin, mitoxantrone, as well as gefitinib.[20] Numerous studies have indicated that ABCG2 is involved in acquired resistance to gefitinib.[19] The level of ABCG2 is upregulated in gefitinib-resistant NSCLC tissues and cell lines, resulting in decreased intracellular gefitinib accumulation.[37,38] However, the mechanisms controlling ABCG2 upregulation in gefitinib-resistant NSCLC are not clear. Our present study suggests for the first time that the expression and function of ABCG2 can be modulated by circSETD3 through the miR-520h sponge.

Finally, we reported that the splicing factor SRSF1 contributed to the upregulation of circSETD3 in gefitinib-resistant NSCLC. In general, circRNAs are produced by spliceosome-mediated pre-mRNA back-splicing.[39] Although the efficiency of back-splicing is much lower than that of linear splicing in human cells, functional alteration of spliceosomal components has been shown to cause preferred circRNA expression.[34,40] SRSF1, as the archetype member of the serine/arginine-rich (SR) protein family of splicing regulators, is a multifunctional protein involved in the regulation of alternative splicing and other processes related to RNA metabolism. In addition, SRSF1 is also a proto-oncogene and plays a central role in tumorigenesis and cancer therapy.[41,42] Therefore, dysregulation of SRSF1 may lead to significant changes in alternative splicing patterns, including back-splicing. Previous studies have indicated that depletion of *Drosophila* splicing factor SF2 (homolog of human SRSF1) facilitates back-splicing from the endogenous *Laccase2* gene, resulting in an increased *Laccase2* circular RNA level and a decreased linear *Laccase2* mRNA level.[43] Consistent with these results, we found that the downregulation of SRSF1 in gefitinib-resistant NSCLC cells resulted in an increased circSETD3 level and a corresponding decreased linear *SETD3* mRNA level, but the underlying mechanisms need further investigation.

SETD3 is a member of the protein lysine methyltransferase (PKMT) family, which catalyzes the addition of methyl group to lysine residues.[44] Recent findings have implicated a role of SETD3 in tumorigenesis and cancer therapy, but its role may vary depending on the cancer type. For instance, SETD3 is upregulated in HCC tissues and positively correlated with proliferation of HCC cells, but it is

**Figure 4. circSETD3 Reduces Gefitinib Sensitivity in NSCLC Cells**

(A) circSETD3 expression in PC9 and HCC827 cells following circSETD3 overexpression. (B) circSETD3 overexpression increased the cell viability of PC9 and HCC827 cells after various concentrations of gefitinib exposure for 48 h. (C) circSETD3 overexpression decreased the cell apoptosis rate of PC9 and HCC827 cells after 1 μM gefitinib exposure for 48 h. (D) circSETD3 expression in PC9/GR and HCC827/GR cells following circSETD3 knockdown. (E) circSETD3 knockdown decreased the cell viability of PC9/GR and HCC827/GR cells after various concentration of gefitinib exposure for 48 h. (F) circSETD3 overexpression increased the cell apoptosis rate of PC9/GR and HCC827/GR cells after 1 μM gefitinib exposure for 48 h. *$p < 0.05$, **$p < 0.01$.

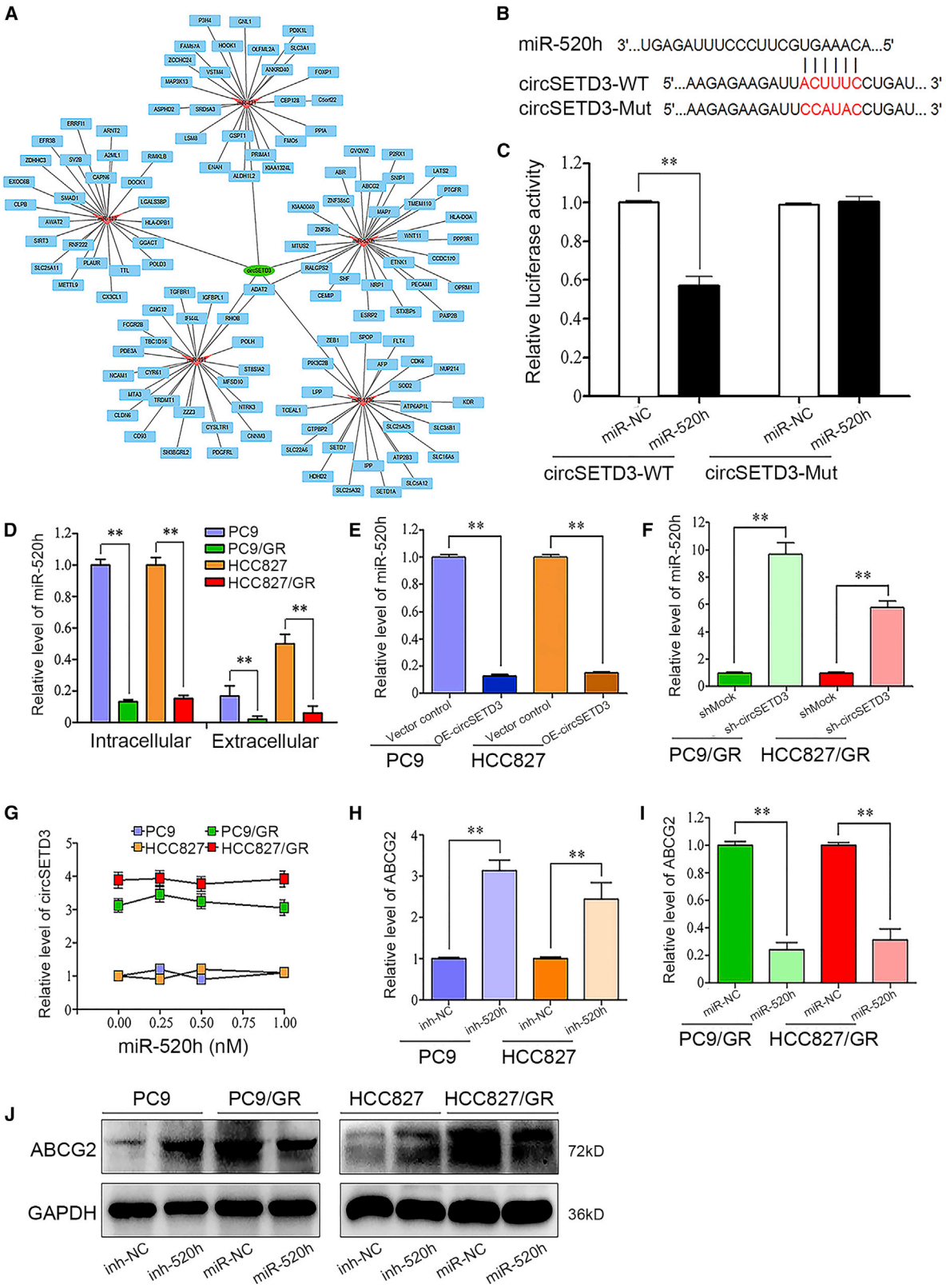


*(legend on next page)*

downregulated in renal cell tumors.[45,46] Moreover, SETD3 has also been indicated to enhance the doxorubicin sensitivity in colon cancer cells and correlate with better survival of colon cancer patients.[44] In the present study, the linear *SETD3* mRNA level was downregulated in gefitinib-resistant NSCLC cells, but the expression of SETD3 protein as well as its function have not yet been clarified and require further study.

## MATERIALS AND METHODS

### Cell Culture and Treatment

Human NSCLC cell lines PC9 and HCC827 (harboring exon 19 deletion of EGFR), as well as HEK293 cells, were obtained from the Cellular Institute of the Chinese Academy of Sciences. Cells were cultured in RPMI 1640 medium (Gibco, Rockville, IN, USA) supplemented with 10% fetal bovine serum, and incubated at 37°C in a humidified atmosphere with 5% $CO_2$ and 95% air. The NSCLC cells with acquired resistance to gefitinib were generated as described previously.[47] The surviving cells were subsequently maintained in the conditioned medium with 1 μM gefitinib (Target Mol, Boston, MA, USA) to retain its drug-resistant phenotype. To eliminate the effects of gefitinib, the resistant cells were cultured in a drug-free medium for at least 2 weeks before all experiments. All lines were regularly tested for mycoplasma.

### Patients and Clinical Sample Collection

This study was approved by the Ethics Committee Board of Chongqing Medical University (no. 2017009) and was registered with the Chinese Clinical Trial Registry (no. ChiCTR1800014660). A total of 30 NSCLC patients who underwent first-line gefitinib therapy, including 15 gefitinib-sensitive patients and 15 acquired gefitinib-resistant patients, were enrolled. Written informed consents were obtained from all of them. The patients were given gefitinib (AstraZeneca, USA) at a daily dose of 250 mg until tumor progression, and the objective response to treatment was assessed with the Response Evaluation Criteria in Solid Tumors (RECIST) version 1.1. Acquired resistance to gefitinib was defined by using the Jackman et al.[48] criteria. Details of patients are listed in Table S3.

Whole blood was collected into tubes containing ethylenediaminetetraacetic acid (EDTA) and centrifuged within 4 h to obtain plasma (2,000 × *g* for 10 min at 4°C). The upper plasma phase was transferred to a new tube without disturbing the intermediate buffy coat layer. Next, the plasma samples were centrifuged (12,000 × *g* for 10 min at 4°C) to remove cellular nucleic acids attached to cell debris, transferred to new tubes, and stored at −80°C until use.

### RNA Preparation

Total RNA was extracted from each specimen using TRIzol reagent (Invitrogen, Life Technologies, Germany) according to the manufacturer's instructions.

For nuclear and cytoplasmic fractions, RNA was extracted using a Paris kit (Invitrogen, Life Technologies, Germany) according to the manufacturer's instructions. The percentages in fractions were analyzed using the following formula: $2^{Ct}$ (nuclear)/$2^{Ct}$ (nuclear) + $2^{Ct}$ (cytoplasm) and $2^{Ct}$ (cytoplasm)/$2^{Ct}$ (nuclear) + $2^{Ct}$ (cytoplasm).

RNA contained in plasma and cell culture supernatants was extracted using a miRNeasy serum/plasma kit (Qiagen, Germany) according to the manufacturer's instructions.

### Small Interfering RNA (siRNA) and circSETD3-Overexpressing Lentivirus

For the transient knockdown of SRSF1, HNRNPK, and HNRNPH1, cells were transfected with 100 nM siRNA or negative control siRNA (siNC) (RiboBio, Guangzhou, China) using Lipo2000 according to the manufacturer's instructions. The efficacy of transfection was verified by a western blot assay. The siRNA sequences are as follows: si-SRSF1, 5′-GUCAUAACTGGAATATGATTT-3′; si-HNRNPK, 5′-UGUGAAGCAGUAUUCUGGAAAGUUU-3′; si-HNRNPH1, 5′-AAUCAGAAGAUGAAGUCAAAUdTdT-3′. Also, siRNAs targeting the junction region of the circSETD3 were designed and synthesized by RiboBio (Guangzhou, China). The sequence of circSETD3 siRNA was 5′-CAUCCAGUCAGAAAAAUGGdTdT-3′. For the stable knockdown of circSETD3, cells were transfected with GV230/EGFP/Neo$^r$ lentivirus encoding sh-circSETD3 or scrambled sequence (shMock) (Genechem, Shanghai, China). Stable cell clones were selected by G418 and then verified by qRT-PCR.

To overexpress circSETD3, cells were infected with OE-circSETD3 or control plasmid (vector control) (Genechem, Guangzhou, China). Stable cell clones were selected by G418 and then verified by qRT-PCR.

### Cell Viability Assay

Cells were seeded in a 96-well plate at a density of 5 × $10^3$ cells per well. After 24 h of incubation, cells were treated with various concentrations of gefitinib (0, 0.01, 0.1, 1, 10, and 100 μM) for 48 h, then 10 μL of CCK-8 solution (Dojindo Molecular Technologies, Japan) was added and incubated for an additional 4 h. The absorbance was measured at 450 nm with a Hitachi F-7000 fluorescence spectrophotometer (Hitachi High-Tech, Japan).

**Figure 5. circSETD3 Acts as a Sponge for miR-520h in NSCLC Cells**

(A) Interaction network of circSETD3-miRNAs-target genes. (B) Binding site of miR-520h with wild-type or mutant circSETD3. (C) The luciferase activity in HEK293 cells transfected with wild-type or mutant circSETD3 and miR-520h mimics or control. (D) The expression of miR-520h was decreased after acquired resistance to gefitinib in NSCLC cells. (E) Levels of miR-520h were reduced after circSETD3 overexpression in PC9 and HCC827 cells. (F) Levels of miR-520h were increased after circSETD3 knockdown in PC9/GR and HCC827/GR cells. (G) Expression change of circSETD3 did not affect the expression of miR-520h. (H) Inhibition of miR-520h in PC9 and HCC827 cells increased the expression of *ABCG2* mRNA. (I) miR-520h mimic reduced the expression of *ABCG2* mRNA in PC9/GR and HCC827/GR cells. (J) ABCG2 levels were increased after miR-520h inhibitor treatment, while they were decreased after miR-520h mimic treatment. *$p < 0.05$, **$p < 0.01$.

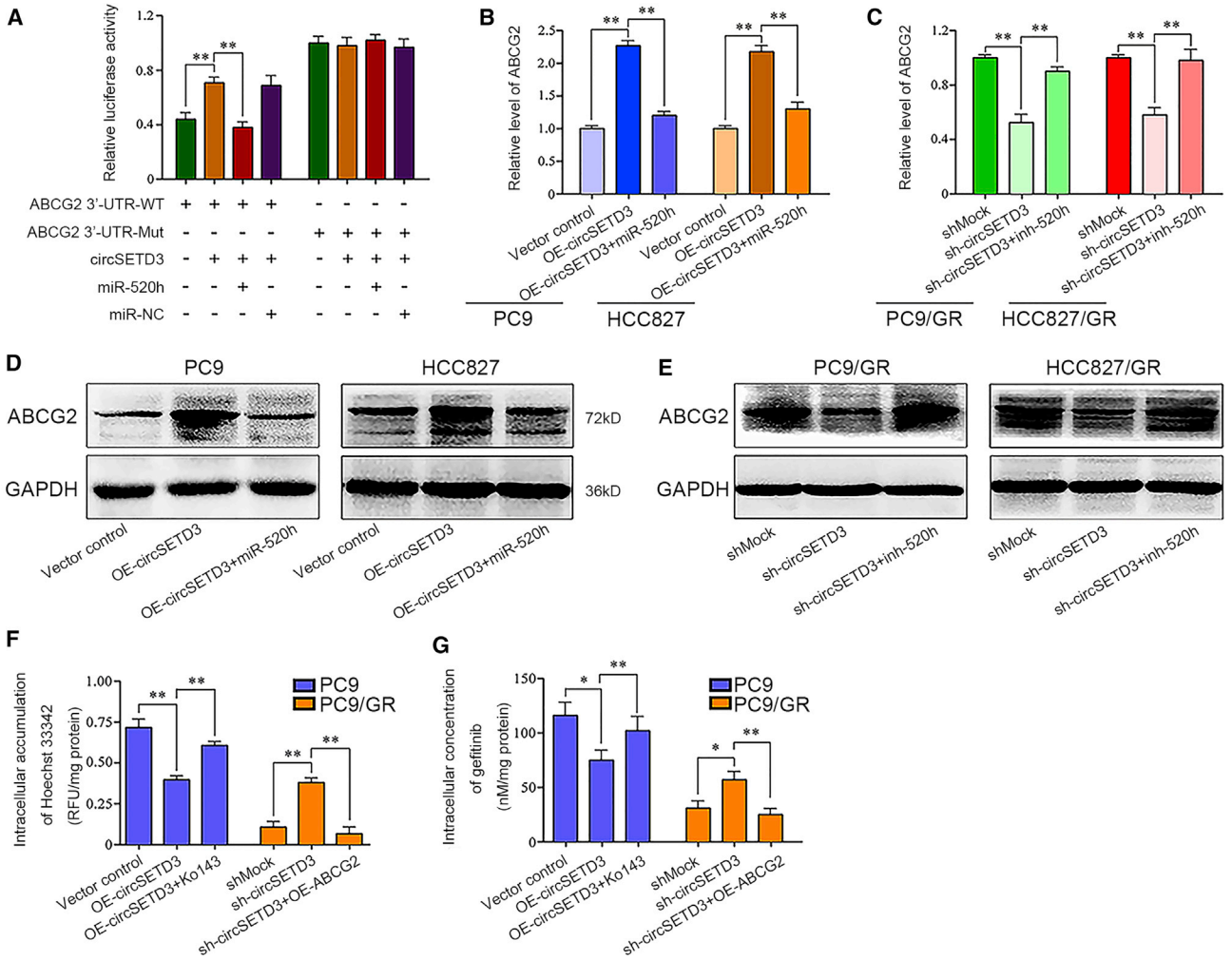


**Figure 6. circSETD3 Influences the Gefitinib Sensitivity through the circSETD3/miR-520h/ABCG2 Pathway**

(A) The luciferase reporter activities of the wild-type ABCG2 3′ UTR were significantly increased in HEK293 cells after transfection with circSETD3, which was reversed by the miR-520h mimic. (B and D) Overexpression of circSETD3 increased the ABCG2 mRNA and protein levels in PC9 and HCC827 cells, which could be abolished by miR-520h mimic. (C and E) Knockdown of circSETD3 decreased the ABCG2 mRNA and protein levels in PC9/GR and HCC827/GR cells, which could be rescued by the miR-520h inhibitor. (F) circSETD3 suppressed the ABCG2-mediated Hoechst 33342 intracellular accumulation in NSCLC cells. (G) circSETD3 suppressed the ABCG2-mediated gefitinib intracellular accumulation in NSCLC cells. *$p < 0.05$, **$p < 0.01$.

### Cell Apoptosis and Cycle Assay

Cells were seeded in a six-well plate at a density of $1 \times 10^5$ cells per well, and treated with 1 μM gefitinib or DMSO for 48 h. For the apoptosis assay, cells were incubated with 5 μL of fluorescein isothiocyanate (FITC)-conjugated annexin V and 5 μL of propidium iodide (PI) for 15 min in the dark at room temperature. For cell cycle assay, cells were fixed with chilled 70% ethanol, then treated with 100 μL of RNase A and stained with 400 μL of PI at 4°C for 30 min in the dark. Cell apoptosis rate and cycling were analyzed using a CytoFLEX flow cytometer (Beckman Coulter, CA, USA).

### Protein Isolation and Western Blot Analysis

Total protein was extracted and quantified using the Pierce bicinchoninic acid (BCA) protein assay kit (Thermo Fisher Scientific, USA). Proteins were separated by 10% SDS-PAGE and transferred to polyvinylidene fluoride (PVDF) membranes. The membrane was blocked with 5% BSA for 1 h and incubated at 4°C overnight with primary antibodies as follows: EGFR (1:1,000, Abcam), phosphorylated (phospho-)EGFR (Tyr1068) (1:500, Abcam), phosphatidylinositol 3-kinase (PI3K) phospho-PI3K (Tyr458/199) (1:1,000, Cell Signaling Technology), Akt (1:1,000, Cell Signaling Technology), phospho-Akt (Ser473) (1:2,000, Cell Signaling Technology), ABCG2 (1:1,000, Bioss), SRSF1 (1:1,000, Bioss), and GAPDH (1:5,000, Bioss). After 1 h of incubation with horseradish peroxidase (HRP)-conjugated secondary antibodies, immunoreactive bands were detected by ECL Prime (GE Healthcare, UK) and an LAS-3000 imager (Fujifilm, Japan).

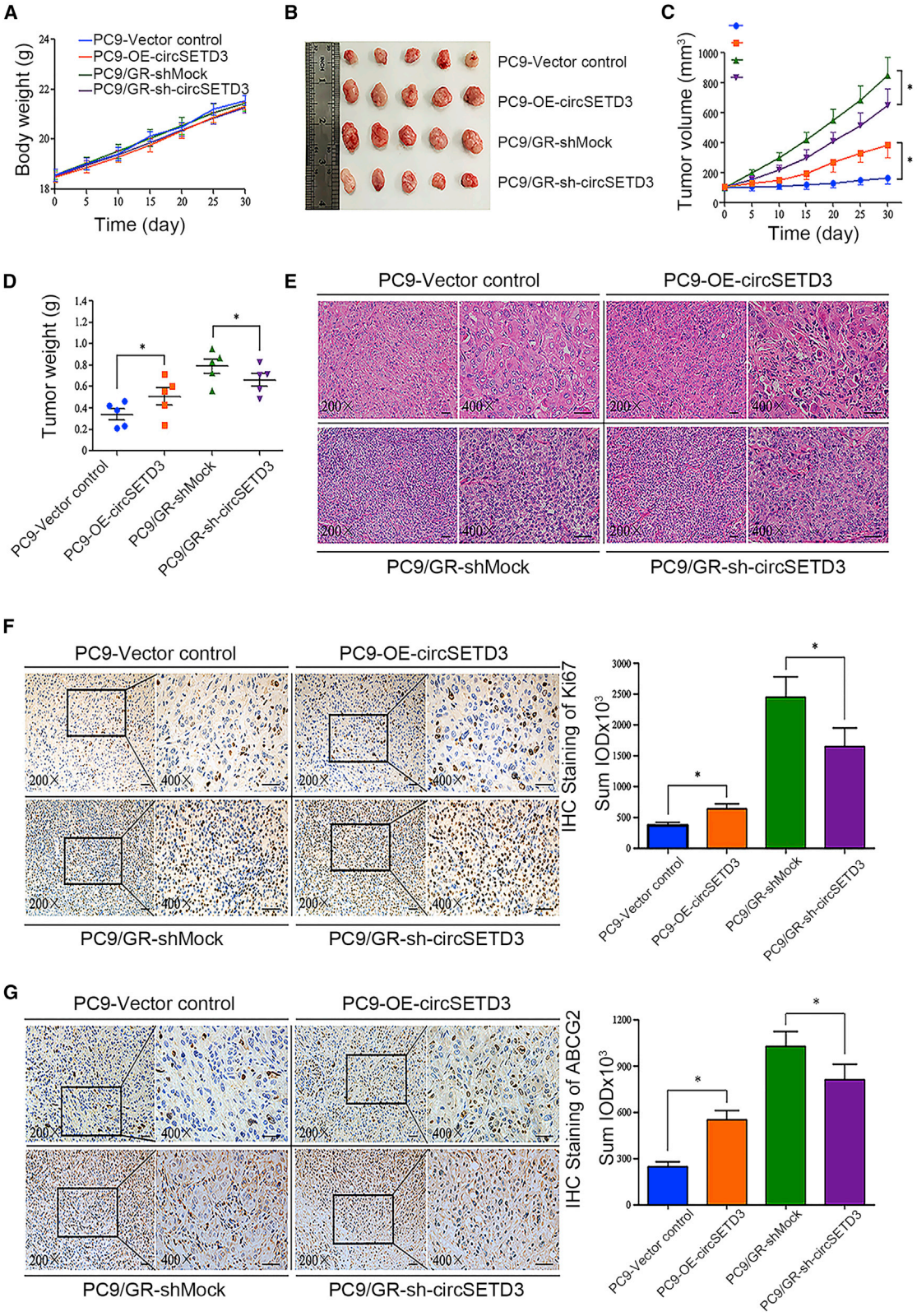


*(legend on next page)*

### RNA-Seq Analysis

Total RNA from NSCLC cells was extracted using TRIzol reagent (Invitrogen, USA) and was treated with the Turbo DNA-free kit (Thermo Fisher Scientific, USA) to degrade the remaining DNA. The RNA was subsequently purified using a Ribo-Zero Gold kit (Illumina, USA) and RNase R (Epicenter, USA). RNA integrity was evaluated using an Agilent 2100 bioanalyzer (Agilent Technologies, Santa Clara, CA, USA). The samples with a RNA integrity number (RIN) $\geq 7$ were subjected to the subsequent analysis. The libraries were constructed using TruSeq stranded total RNA with Ribo-Zero Gold according to the manufacturer's instructions. Then, these libraries were sequenced on the Illumina sequencing platform (HiSeq 2500 or other platform), and 150-bp/125-bp paired-end reads were generated. All of the sequencing procedures and analyses were performed in OEbiotech (Shanghai, China). The criteria for differential circRNA expression included a fold change $\geq 2$ or $\leq 0.5$ between compared groups and statistical significance at $p < 0.05$ as well as the false discovery rate <0.05.

### Quantitative Real-Time PCR

The separation of the nuclear and cytoplasmic RNA was performed using a Paris kit (Thermo Fisher Scientific, Waltham, MA, USA). Total RNA from whole-cell lysate was isolated with TRIzol reagent. Total RNA from cell culture medium and plasma of patients were isolated using a miRNeasy serum/plasma kit (Qiagen, CA, USA). For RNase R treatment, 2 μg of total RNA was incubated for 20 min at 37°C with or without 3 U/μg of RNase R (Epicenter Technologies, Madison, WI, USA), and the resulting RNA was subsequently purified using a RNeasy MinElute cleanup kit (Qiagen, Valencia, CA, USA). A total of 1 μg of RNA was reverse transcribed into cDNA using the PrimeScript RT reagent kit (TaKaRa Bio, Shiga, Japan). Quantitative real-time PCR was performed using SYBR Premix Ex Taq II (Takara Bio, Shiga, Japan) according to the manufacturer's instruction. The primer sequences used in this study are shown in Table S4. Relative expression levels were analyzed using the $2^{-\Delta\Delta Ct}$ method as a ratio relative to the *U6* or *GAPDH* levels in each sample.[49]

### Luciferase Reporter Assay

The wild-type or mutant sequences of circSETD3 and *ABCG2* containing the putative miR-520h binding sites were subcloned into psiCHECK-2 vector (Promega, Madison, WI, USA). HEK293 cells were co-transfected with psiCHECK-2 dual-luciferase vector with or without miR-520h mimic, miR-520h inhibitor, or circSETD3 overexpression plasmid. The luciferase activity was measured with a dual-luciferase reporter assay system (Promega, Madison, WI, USA).

### Measurement of Intracellular Hoechst 33342 and Gefitinib Accumulation

Cells were seeded into six-well plates at a density of $5 \times 10^5$ cells per well for 48 h before Hoechst 33342 (5 μg/mL) or gefitinib (1 μM) was added. After 1 h of incubation, the intracellular fluorescence intensity of Hoechst 33342 was measured using BD Influx (BD Biosciences, Franklin Lakes, NJ, USA) by the setting of excitation with a 350-nm ultraviolet laser and detection through a 460/50-nm bandpass filter. After 6 h of incubation, the intracellular gefitinib was extracted and measured by the liquid chromatography-tandem mass spectrometry (LC-MS/MS) method as described previously.[47]

### NSCLC Xenograft Mice Models

All animal experiments were approved by the Animal Ethics and Experimental Committee of the Chongqing Medical University and performed according to the National Institutes of Health *Guide for the Care and Use of Laboratory Animals*. BALB/c-nude mice (females, 4–6 weeks, 16–20 g) were randomized into four groups (n = 5) and subjected to subcutaneous injection with the circSETD3-overexpressing PC9 cells (PC9-OE-circSETD3), empty-vector transfected PC9 cells (PC9-vector control), circSETD3-knockdown PC9/GR cells (PC9/GR-sh-circSETD3), or shMock-transfected PC9/GR cells (PC9/GR-shMock) ($5 \times 10^6$ cells/mouse) in each right flank. When all tumors reached a mean volume of 100 $mm^3$, the mice were treated with gefitinib (30 mg/kg/day) for 30 days by oral gavage. Investigators were not blinded to mouse treatment conditions at the time of measurement. At the end of experiments, mice were sacrificed and the tumors were removed for examination of the parameters of interest.

### Immunohistochemical Analysis

Xenografts were fixed in 4% paraformaldehyde, embedded in paraffin, and cut at a thickness of 4 μm. The sections were deparaffinized in xylene and incubated with the primary antibodies (Ki-67, 1:100 dilution, Abcam; ABCG2, 1:1,000 dilution, Abcam) overnight at 4°C. Three slides per groups were observed under a standard light microscope (BX53, Olympus). In each section, 10 areas were randomly selected and scored for the positive cells using an automated image analysis system (Visiomorph, Visiopharm Integrator System, Denmark).

### Statistical Analysis

Statistical analyses were performed using SPSS 20.0 (IBM, USA) and GraphPad Prism version 6.0 (GraphPad, San Diego, CA, USA). All data were verified in three independent experiments and were summarized as means ± standard deviation (SD), with similar variance between all groups being compared. One-way ANOVA and a two-tailed Student's t test were performed to analyze the differences between sets of data. The 30 patients with NSCLC were divided into

**Figure 7. circSETD3 Reduces Gefitinib Sensitivity in Xenograft Tumor Models**

(A) Average body weight curves of mice in different groups. (B–D) Tumor growth in different groups after treatment with gefitinib (30 mg/kg/day after tumors reached a mean volume of 100 $mm^3$ for 30 days by oral gavage). PC9-OE-circSETD3 tumors are significantly bigger than PC9-Vector control tumors and PC9/GR-sh-circSETD3 tumors are significantly smaller than PC9/GR-shMock tumors. (E) H&E staining in xenograft tumors. (F and G) Representative immunohistochemical staining of (F) Ki-67 and (G) ABCG2 in xenograft tumors. Scale bars, 50 μm. *$p < 0.05$.

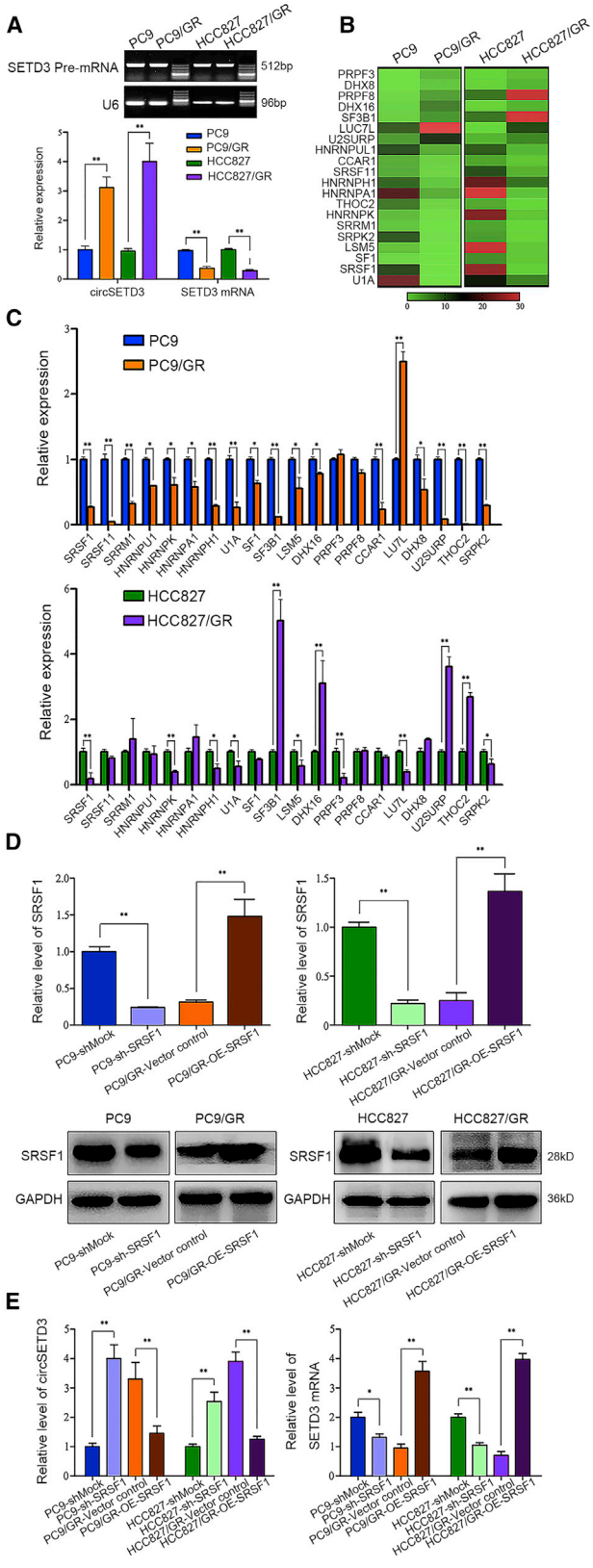


**Figure 8. SRSF1 Upregulates circSETD3 Expression in the Development of Resistance to Gefitinib in NSCLC Cells**

(A) The expression of SETD3 pre-mRNA and linear SETD3 mRNA in gefitinib-sensitive and -resistant NSCLC cells. (B) Differentially expressed splicing factors between gefitinib-sensitive and -resistant NSCLC cells with RNA-seq. (C) Quantitative real-time PCR validation of the selected splicing factors expression. (D) SRSF1 expression in NSCLC cells following overexpression or knockdown. (E) The influence of SRSF1 on the expression of circSETD3 and linear SETD3 mRNA. *$p < 0.05$, **$p < 0.01$.

high (n = 12) and low (n = 18) circSETD3 expression groups according to Youden's index.[50,51] Values of $p < 0.05$ were considered statistically significant.

## SUPPLEMENTAL INFORMATION

Supplemental Information can be found online at https://doi.org/10.1016/j.omtn.2020.07.027.

## AUTHOR CONTRIBUTIONS

Y.H. and Y.D. performed and analyzed most of the experiments. C.W. and S.H. assisted with data analysis, while J.S. and D.Z. helped obtain the experimental data. L.W. and Y.H. wrote the manuscript. L.W. provided all financial support and critical intellectual input in the study design and manuscript preparation. H.Z. and L.W. revised the paper. All authors discussed the results and commented on the manuscript. All authors read and approved the final manuscript.

## CONFLICTS OF INTEREST

The authors declare no competing interests.

## ACKNOWLEDGMENTS

The authors thank Chang Chen (Institute of Life Sciences, Chongqing Medical University, Chongqing, China) for LC-MS/MS experiments. This work was supported by the National Scientific Foundation of China (nos. 81473284 and 81603201).

## REFERENCES

1. Bray, F., Ferlay, J., Soerjomataram, I., Siegel, R.L., Torre, L.A., and Jemal, A. (2018). Global cancer statistics 2018: GLOBOCAN estimates of incidence and mortality worldwide for 36 cancers in 185 countries. CA Cancer J. Clin. *68*, 394–424.

2. Provencio, M., Sánchez, A., Garrido, P., and Valcárcel, F. (2010). New molecular targeted therapies integrated with radiation therapy in lung cancer. Clin. Lung Cancer *11*, 91–97.

3. Tas, F., Ciftci, R., Kilic, L., and Karabulut, S. (2013). Age is a prognostic factor affecting survival in lung cancer patients. Oncol. Lett. *6*, 1507–1513.

4. Ennis, B.W., Lippman, M.E., and Dickson, R.B. (1991). The EGF receptor system as a target for antitumor therapy. Cancer Invest. *9*, 553–562.

5. Jutten, B., and Rouschop, K.M. (2014). EGFR signaling and autophagy dependence for growth, survival, and therapy resistance. Cell Cycle *13*, 42–51.

6. Salomon, D.S., Brandt, R., Ciardiello, F., and Normanno, N. (1995). Epidermal growth factor-related peptides and their receptors in human malignancies. Crit. Rev. Oncol. Hematol. *19*, 183–232.

7. Solassol, I., Pinguet, F., and Quantin, X. (2019). FDA- and EMA-approved tyrosine kinase inhibitors in advanced *EGFR*-mutated non-small cell lung cancer: safety, tolerability, plasma concentration monitoring, and management. Biomolecules *9*, E668.

8. Gandara, D.R., Li, T., Lara, P.N., Kelly, K., Riess, J.W., Redman, M.W., and Mack, P.C. (2014). Acquired resistance to targeted therapies against oncogene-driven non-small-

cell lung cancer: approach to subtyping progressive disease and clinical implications. Clin. Lung Cancer *15*, 1–6.

9. Majem, M., and Remon, J. (2013). Tumor heterogeneity: evolution through space and time in EGFR mutant non small cell lung cancer patients. Transl. Lung Cancer Res. *2*, 226–237.
10. Morgillo, F., Della Corte, C.M., Fasano, M., and Ciardiello, F. (2016). Mechanisms of resistance to EGFR-targeted drugs: lung cancer. ESMO Open *1*, e000060.
11. Bolha, L., Ravnik-Glavač, M., and Glavač, D. (2017). Circular RNAs: biogenesis, function, and a role as possible cancer biomarkers. Int. J. Genomics *2017*, 6218353.
12. Arnaiz, E., Sole, C., Manterola, L., Iparraguirre, L., Otaegui, D., and Lawrie, C.H. (2019). circRNAs and cancer: biomarkers and master regulators. Semin. Cancer Biol. *58*, 90–99.
13. Barrett, S.P., and Salzman, J. (2016). Circular RNAs: analysis, expression and potential functions. Development *143*, 1838–1847.
14. Huang, X., Li, Z., Zhang, Q., Wang, W., Li, B., Wang, L., Xu, Z., Zeng, A., Zhang, X., Zhang, X., et al. (2019). Circular RNA AKT3 upregulates PIK3R1 to enhance cisplatin resistance in gastric cancer via miR-198 suppression. Mol. Cancer *18*, 71.
15. Kun-Peng, Z., Xiao-Long, M., and Chun-Lin, Z. (2018). Overexpressed circPVT1, a potential new circular RNA biomarker, contributes to doxorubicin and cisplatin resistance of osteosarcoma cells by regulating ABCB1. Int. J. Biol. Sci. *14*, 321–330.
16. Ping, L., Jian-Jun, C., Chu-Shu, L., Guang-Hua, L., and Ming, Z. (2019). High circ_100053 predicts a poor outcome for chronic myeloid leukemia and is involved in imatinib resistance. Oncol. Res. Published online February 14, 2019. 10.3727/096504018X15412701483326.
17. Xue, M., Li, G., Fang, X., Wang, L., Jin, Y., and Zhou, Q. (2019). hsa_circ_0081143 promotes cisplatin resistance in gastric cancer by targeting miR-646/CDK6 pathway. Cancer Cell Int. *19*, 25.
18. Xu, C., Zheng, Y., Lian, D., Ye, S., Yang, J., and Zeng, Z. (2015). Analysis of microRNA expression profile identifies novel biomarkers for non-small cell lung cancer. Tumori *101*, 104–110.
19. Chen, Y.J., Huang, W.C., Wei, Y.L., Hsu, S.C., Yuan, P., Lin, H.Y., Wistuba, I.I., Lee, J.J., Yen, C.J., Su, W.C., et al. (2011). Elevated BCRP/ABCG2 expression confers acquired resistance to gefitinib in wild-type EGFR-expressing cells. PLoS ONE *6*, e21428.
20. Galetti, M., Petronini, P.G., Fumarola, C., Cretella, D., La Monica, S., Bonelli, M., Cavazzoni, A., Saccani, F., Caffarra, C., Andreoli, R., et al. (2015). Effect of ABCG2/BCRP expression on efflux and uptake of gefitinib in NSCLC cell lines. PLoS ONE *10*, e0141795.
21. Gout, S., Brambilla, E., Boudria, A., Drissi, R., Lantuejoul, S., Gazzeri, S., and Eymin, B. (2012). Abnormal expression of the pre-mRNA splicing regulators SRSF1, SRSF2, SRPK1 and SRPK2 in non small cell lung carcinoma. PLoS ONE *7*, e46539.
22. Shi, J., Huang, Y., Wen, C., He, S., Wu, L., and Zhou, H. (2020). Genome-wide identification and characterization of long non-coding RNAs involved in acquired resistance to gefitinib in non-small-cell lung cancer. Comput. Biol. Chem. *87*, 107288.
23. Lee, A.F., Chen, M.C., Chen, C.J., Yang, C.J., Huang, M.S., and Liu, Y.P. (2017). Reverse epithelial-mesenchymal transition contributes to the regain of drug sensitivity in tyrosine kinase inhibitor-resistant non-small cell lung cancer cells. PLoS ONE *12*, e0180383.
24. Cheng, H., Ge, X., Zhuo, S., Gao, Y., Zhu, B., Zhang, J., Shang, W., Xu, D., Ge, W., and Shi, L. (2018). β-Elemene synergizes with gefitinib to inhibit stem-like phenotypes and progression of lung cancer via down-regulating EZH2. Front. Pharmacol. *9*, 1413.
25. Memczak, S., Jens, M., Elefsinioti, A., Torti, F., Krueger, J., Rybak, A., Maier, L., Mackowiak, S.D., Gregersen, L.H., Munschauer, M., et al. (2013). Circular RNAs are a large class of animal RNAs with regulatory potency. Nature *495*, 333–338.
26. Shen, Q., Yao, Q., Sun, J., Feng, L., Lu, H., Ma, Y., Liu, L., Wang, F., Li, J., Yue, Y., et al. (2014). Downregulation of histone deacetylase 1 by microRNA-520h contributes to the chemotherapeutic effect of doxorubicin. FEBS Lett. *588*, 184–191.
27. Su, C.M., Wang, M.Y., Hong, C.C., Chen, H.A., Su, Y.H., Wu, C.H., Huang, M.T., Chang, Y.W., Jiang, S.S., Sung, S.Y., et al. (2016). miR-520h is crucial for DAPK2 regulation and breast cancer progression. Oncogene *35*, 1134–1142.
28. Zhang, J., Liu, W., Shen, F., Ma, X., Liu, X., Tian, F., Zeng, W., Xi, X., and Lin, Y. (2018). The activation of microRNA-520h-associated TGF-β1/c-Myb/Smad7 axis promotes epithelial ovarian cancer progression. Cell Death Dis. *9*, 884.
29. Wang, F., Xue, X., Wei, J., An, Y., Yao, J., Cai, H., Wu, J., Dai, C., Qian, Z., Xu, Z., and Miao, Y. (2010). hsa-miR-520h downregulates ABCG2 in pancreatic cancer cells to inhibit migration, invasion, and side populations. Br. J. Cancer *103*, 567–574.
30. Beretta, G.L., Cassinelli, G., Pennati, M., Zuco, V., and Gatti, L. (2017). Overcoming ABC transporter-mediated multidrug resistance: the dual role of tyrosine kinase inhibitors as multitargeting agents. Eur. J. Med. Chem. *142*, 271–289.
31. Scharenberg, C.W., Harkey, M.A., and Torok-Storb, B. (2002). The ABCG2 transporter is an efficient Hoechst 33342 efflux pump and is preferentially expressed by immature human hematopoietic progenitors. Blood *99*, 507–512.
32. Allen, J.D., van Loevezijn, A., Lakhai, J.M., van der Valk, M., van Tellingen, O., Reid, G., Schellens, J.H., Koomen, G.J., and Schinkel, A.H. (2002). Potent and specific inhibition of the breast cancer resistance protein multidrug transporter in vitro and in mouse intestine by a novel analogue of fumitremorgin C. Mol. Cancer Ther. *1*, 417–425.
33. Kristensen, L.S., Hansen, T.B., Venø, M.T., and Kjems, J. (2018). Circular RNAs in cancer: opportunities and challenges in the field. Oncogene *37*, 555–565.
34. Liang, D., Tatomer, D.C., Luo, Z., Wu, H., Yang, L., Chen, L.-L., Cherry, S., and Wilusz, J.E. (2017). The output of protein-coding genes shifts to circular RNAs when the pre-mRNA processing machinery is limiting. Mol. Cell *68*, 940–954.e3.
35. Shang, J., Chen, W.M., Wang, Z.H., Wei, T.N., Chen, Z.Z., and Wu, W.B. (2019). circPAN3 mediates drug resistance in acute myeloid leukemia through the miR-153-5p/miR-183-5p-XIAP axis. Exp. Hematol. *70*, 42–54.e3.
36. Xu, L., Feng, X., Hao, X., Wang, P., Zhang, Y., Zheng, X., Li, L., Ren, S., Zhang, M., and Xu, M. (2019). circSETD3 (hsa_circ_0000567) acts as a sponge for microRNA-421 inhibiting hepatocellular carcinoma growth. J. Exp. Clin. Cancer Res. *38*, 98.
37. Ozvegy-Laczka, C., Hegedus, T., Várady, G., Ujhelly, O., Schuetz, J.D., Váradi, A., Kéri, G., Orfi, L., Német, K., and Sarkadi, B. (2004). High-affinity interaction of tyrosine kinase inhibitors with the ABCG2 multidrug transporter. Mol. Pharmacol. *65*, 1485–1495.
38. Toyoda, Y., Takada, T., and Suzuki, H. (2019). Inhibitors of human ABCG2: from technical background to recent updates with clinical implications. Front. Pharmacol. *10*, 208.
39. Wang, Y., and Wang, Z. (2015). Efficient backsplicing produces translatable circular mRNAs. RNA *21*, 172–179.
40. Zhang, Y., Xue, W., Li, X., Zhang, J., Chen, S., Zhang, J.L., Yang, L., and Chen, L.L. (2016). The biogenesis of nascent circular RNAs. Cell Rep. *15*, 611–624.
41. Das, S., and Krainer, A.R. (2014). Emerging functions of SRSF1, splicing factor and oncoprotein, in RNA metabolism and cancer. Mol. Cancer Res. *12*, 1195–1204.
42. Sheng, J., Zhao, Q., Zhao, J., Zhang, W., Sun, Y., Qin, P., Lv, Y., Bai, L., Yang, Q., Chen, L., et al. (2018). SRSF1 modulates PTPMT1 alternative splicing to regulate lung cancer cell radioresistance. EBioMedicine *38*, 113–126.
43. Kramer, M.C., Liang, D., Tatomer, D.C., Gold, B., March, Z.M., Cherry, S., and Wilusz, J.E. (2015). Combinatorial control of *Drosophila* circular RNA expression by intronic repeats, hnRNPs, and SR proteins. Genes Dev. *29*, 2168–2182.
44. Abaev-Schneiderman, E., Admoni-Elisha, L., and Levy, D. (2019). SETD3 is a positive regulator of DNA-damage-induced apoptosis. Cell Death Dis. *10*, 74.
45. Cheng, X., Hao, Y., Shu, W., Zhao, M., Zhao, C., Wu, Y., Peng, X., Yao, P., Xiao, D., Qing, G., et al. (2017). Cell cycle-dependent degradation of the methyltransferase SETD3 attenuates cell proliferation and liver tumorigenesis. J. Biol. Chem. *292*, 9022–9033.
46. Pires-Luís, A.S., Vieira-Coimbra, M., Vieira, F.Q., Costa-Pinheiro, P., Silva-Santos, R., Dias, P.C., Antunes, L., Lobo, F., Oliveira, J., Gonçalves, C.S., et al. (2015). Expression of histone methyltransferases as novel biomarkers for renal cell tumor diagnosis and prognostication. Epigenetics *10*, 1033–1043.
47. Zhao, H., Huang, Y., Shi, J., Dai, Y., Wu, L., and Zhou, H. (2018). ABCC10 plays a significant role in the transport of gefitinib and contributes to acquired resistance to gefitinib in NSCLC. Front. Pharmacol. *9*, 1312.
48. Jackman, D., Pao, W., Riely, G.J., Engelman, J.A., Kris, M.G., Jänne, P.A., Lynch, T., Johnson, B.E., and Miller, V.A. (2010). Clinical definition of acquired resistance to

epidermal growth factor receptor tyrosine kinase inhibitors in non-small-cell lung cancer. J. Clin. Oncol. *28*, 357–360.

49. Livak, K.J., and Schmittgen, T.D. (2001). Analysis of relative gene expression data using real-time quantitative PCR and the $2^{-\Delta\Delta C(T)}$ method. Methods *25*, 402–408.

50. Fluss, R., Faraggi, D., and Reiser, B. (2005). Estimation of the Youden index and its associated cutoff point. Biom. J. *47*, 458–472.

51. Wanneh, E., Luna, G., Dufour, R., and Baass, A. (2017). Predicting proprotein convertase subtilisin kexin type-9 loss of function mutations using plasma PCSK9 concentration. J. Clin. Lipidol. *11*, 55–60.